Journal of Materials Chemistry C

Optical Features of Hybrid Molecular/Biological-Quantum Dot Systems Governed by Energy Transfer Processes

Journal:	*Journal of Materials Chemistry C*
Manuscript ID	TC-REV-01-2019-000232.R1
Article Type:	Review Article
Date Submitted by the Author:	12-Apr-2019
Complete List of Authors:	Wax, Terianna; University of Connecticut, Department of Chemistry Zhao, Jing; University of Connecticut, Chemistry

Optical Features of Hybrid Molecular/Biological-Quantum Dot Systems Governed by Energy Transfer Processes

Terianna J. Wax[†] *and Jing Zhao*[†,#,*]

[†]Department of Chemistry, University of Connecticut, 55 North Eagleville Rd., Storrs, CT, 06269-3060, USA

[#]Institute of Materials Science, University of Connecticut, 97 North Eagleville Rd., Storrs, CT, 06269-3136, USA

ABSTRACT: Energy transfer processes are continually being explored in both molecular and biological systems that are coupled to colloidal quantum dots (QDs). Quantum dots display unique size and composition dependent photophysical properties. The conjoining of QDs with various molecular and biological components has led to the development of a range of hybrid materials for energy-related applications. These hybrid systems vary in complexity from those composed of QDs and dyes to that of intricate assemblies of QDs with different proteins and light-harvesting complexes. The optical profiles of these systems such as absorption, emission, and fluorescence lifetime are often influenced by energy transfer processes. In this Review, we discuss the evolving field of molecular/biological-QD systems and enumerate on the interesting optical features these systems exhibit due to energy transfer. We also provide our perspective on the challenges and future directions that are worthy of investigation in this field.

1. INTRODUCTION

The field of nanotechnology encompasses various aspects of material science research, such as exploring the interface between inorganic nanomaterial components with that of molecular and biological systems. These hybrid systems have been extensively studied in a plethora of applications, including solar cells,[1] light emitting devices,[2, 3] bio-imaging probes,[4] and sensors.[5, 6] Specifically, meteoric advancements have been made in the field of energy conversion and storage using hybrid nanosystems. One such inorganic nanomaterial of these hybrid systems is colloidal quantum dots (QDs). Colloidal QDs are nanoscale semiconductor crystals that exhibit multiple advantageous optical properties over that of the traditionally used organic fluorophores, such as broad absorption, narrow emission, and high photostability. In addition, the absorption and emission spectra of QDs can be conveniently tuned by changing their size and composition in the synthesis. When conjugated with molecular and biological components, the optical properties of the QD-based hybrid nanomaterials can be further adjusted for energy applications.[7-10] In addition to these applications, interest has also been placed on fundamental processes that modulate the optical properties of the hybrid systems, such as energy transfer mechanisms.[11-13] To optimize energy transfer in these systems for desired applications, it is paramount to understand how energy transfer in hybrid systems influences the physical characteristics of the single elements, such as the absorption and photoluminescent properties of QDs. Furthermore, it is well-known that QDs can also transfer electrons to nearby electron acceptors with good efficiency, making them promising catalysts for photochemistry. Although this type of work is beyond the scope of this Review, we encourage the readers to peruse the recently published Viewpoint from the Weiss group on the prospects of integrating QDs as photocatalysts in light-driven devices.[14] We have included additional references therein for readers interested in learning more on this topic.[15-18]

The evolution of the bio-nanotechnology field has resulted in a growing interest to explore the interaction between QDs and various organic and biological materials. The organic components in these hybrid assemblies can range from small molecules to proteins. QD-molecule/protein systems are promising platforms for biological sensing and imaging, which has been discussed previously.[19-23] There has also been a number of comprehensive reviews that have concentrated on how the physical properties (i.e., size, distance, shape, or ligand encapsulation) of QDs influence energy transfer within a molecular system.[17, 24, 25] Unlike in previous reviews, this Review focuses on the optical properties and energy transfer processes in QD-based hybrid nanostructures with potential applications in an energy-related field. The importance of energy transfer-related studies stems from an interest in emulating the process of photosynthesis. Sunlight provides the most abundant source of energy for earth leading many researchers to investigate how to efficiently harvest solar energy. The natural conversion of solar energy to promote various biological processes is strongly contingent upon the electronic energy transfer from excited donor to acceptor molecules that exist in nature.[26] Hence, a greater understanding of these systems is crucial to improve upon photon capture and energy transfer in hybrid QD/molecular assemblies for potential use in biomimetic applications.

In this Review, we first provide an overview of the Förster resonance energy transfer (FRET), Dexter energy transfer (DET) and triplet-triplet energy transfer (TTET) mechanisms. Second, we concentrate on the coupling between QDs and small molecules, such as J-aggregates and organic dyes, and examine energy transfer processes in these systems. Third, we explore more sophisticated QD heterostructures, in which either light harvesting complexes or proteins are anchored to the QDs. In the final section of this Review, we offer our insight into future directions on energy transfer studies and in designing QD/protein systems.

2. ENERGY TRANSFER PROCESSES IN HETERONANOSTRUCTURES

The coupling of QDs within various molecular and biological contexts results in the change of the optical properties of QDs and the molecules via different energy transfer mechanisms. The most comprehensively investigated energy transfer process to date is Förster resonance energy transfer, or FRET. There has been a myriad of QD-based FRET studies in which QDs have been paired with fluorescent dyes, proteins, enzymes, etc., reported in the literature.[27-31] Although the FRET mechanism has played a pivotal role in governing the optical properties of complexed QD heteroassemblies, the prospect of energy transfer via electron exchange occurring in these systems should not be overlooked. In particular, electron exchange via the Dexter energy transfer (DET) process has been observed between QDs coupled to small molecules, such as ruthenium, ferrocene, quinones, etc.[32-34] Unlike FRET-based applications that are strongly dependent on quantitative optical features (i.e., overlap of absorption and emission spectra of the donor and acceptor molecules),[35-37] DET is contingent on more nuanced factors, such as energy level alignment and the surface properties of the individual components. The following sub-sections of this Review provide a foundation for the FRET and DET mechanisms, in addition to introducing the processes of nanometal surface energy transfer (NSET) and triplet-triplet energy transfer (TTET).

2.1 Förster Resonance Energy Transfer

Förster resonance energy transfer (FRET) was discovered over 100 years ago by Theodor Förster .[38, 39] FRET is a distance-dependent event that entails a nonradiative energy transfer process between an excited fluorophore (donor) and another molecule (acceptor) via a long-range dipole-dipole coupling. In order for FRET to occur between two species, certain guidelines must be fulfilled. The FRET rate (k_{FRET}), or the probability of FRET to occur between a donor and an acceptor over time, is defined by Equation 1

$$k_{FRET} = \tau_D^{-1} \left(\frac{R_0}{r}\right)^6 \quad (1)$$

where τ_D^{-1} is the inverse of the photoluminescence lifetime of the donor without the influence of FRET, R_0 is the Förster distance, and r is the distance between the donor and acceptor molecules. In order for FRET to occur, the proximity between the donor and acceptor molecules should vary between 10 – 100 Å. Furthermore, the efficiency of FRET (E_{FRET}) is dependent upon the inverse sixth-distance between the donor and acceptor as shown in Equation 2.

$$E_{FRET} = \frac{R_0^6}{R_0^6 + r^6} \quad (2)$$

Concomitant with the distance-dependent nature of FRET, optimal spectral overlap between the acceptor absorption and donor emission spectra is crucial to achieve high FRET efficiencies in hybrid systems, which determines R_0. The Förster distance, R_0, is defined by Equation 3 and is the distance at which the excited state donor transfers 50% of its energy to the accepting molecule or emits 50% fluorescence.

$$R_{0(FRET)} = 0.02108[n^{-4}\Phi_d \kappa^2 J]^{1/6} \quad (3)$$

In Equation 3, n is the refractive index of the sample, Φ_d is the quantum yield of the donor molecule, κ^2 is the orientation factor for the transition dipoles, and J is the overlap integral. Moreover, since FRET is dependent upon dipole coupling, the transition dipole orientations of the donor and acceptor must be approximately parallel to one another in order for FRET to occur within a system.

2.2 Nanometal Surface Energy Transfer

In classical FRET systems, the average orientation factor (κ^2) is considered to be $\frac{2}{3}$ for randomly oriented transition dipoles.[40, 41] The orientation factor of $\frac{2}{3}$ can be used in QD-based systems when the synthesized QDs are perfectly spherical, meaning that symmetric QDs exhibit isotropic transition dipoles.[42, 43] However, the alignment of transition dipoles in hybrid QD assemblies is often complexed due to the anisotropic nature of the transition dipoles when synthesized QDs are aspherical in shape. Hence, the equations related to FRET cannot always be applied when investigating energy transfer in QD heteroassemblies. Moreover, studies have unveiled that, for QD/nanoparticle (NP) systems, the rate of FRET does not always follow the d^{-6} distance-dependent relationship between the donor-acceptor pair. For example, Li and coworkers demonstrated a d^{-4} distance dependence quenching of QD photoluminescence when QDs were coupled to ~3 nm gold (Au) NPs.[44] Unlike the FRET formalism that entails a resonant coupling between donor and acceptor, this QD photoluminescence quenching was ascribed to the interaction of oscillating dipoles near the Au surface as a result of nanometal surface energy transfer, or NSET.

The NSET mechanism details a long-range, distance-dependent relationship between QDs and metal NPs similar to FRET, however NSET accounts for the coupling of dipoles located near a metallic surface. In other words, the QD is treated as a transition point dipole, while a smaller sized Au NP (~3 nm) is considered as an infinite metal surface. The NSET study conducted by Li *et al.* demonstrated a size-dependent energy transfer relationship between QDs and Au NPs. CdSe/ZnS QDs were coupled to Au NPs that were either 3, 15, or 80 nm in diameter. Their findings indicated that QDs anchored to the 15 or 80 nm Au NPs followed FRET, while the energy transfer between QDs and 3 nm Au NPs was due to NSET. Energy transfer based on the NSET formalism

has also been investigated over longer intermolecular distances ($R_0 \geq 50$ nm). As opposed to conventional FRET systems in which R_0 is within 2 – 6 nm, the NSET mechanism can be applied as a long-range spectroscopic ruler between a donor and an acceptor.[45, 46] Work conducted by Samanta and coworkers[47] observed NSET-like energy transfer between Au NPs and CdTe/CdS QDs self-assembled on DNA scaffolds. By modulating the distance between the Au NPs and QDs from 15 to 70 nm on the DNA, a long-range quenching in the QD emission was observed, thus demonstrating the potential of the NSET mechanism as a spectroscopic ruler technique.

2.3 Dexter Energy Transfer

Dexter energy transfer (DET) was first theoretically proposed by D. L. Dexter in 1953.[48] Unlike FRET, DET is a short-range energy transfer event that involves the nonradiative exchange of an electron from the excited state donor to the ground state acceptor molecule and is strongly dependent on the energy level alignment of the donor/acceptor pair. Figure 1 illustrates the difference between the FRET and DET processes.[49]

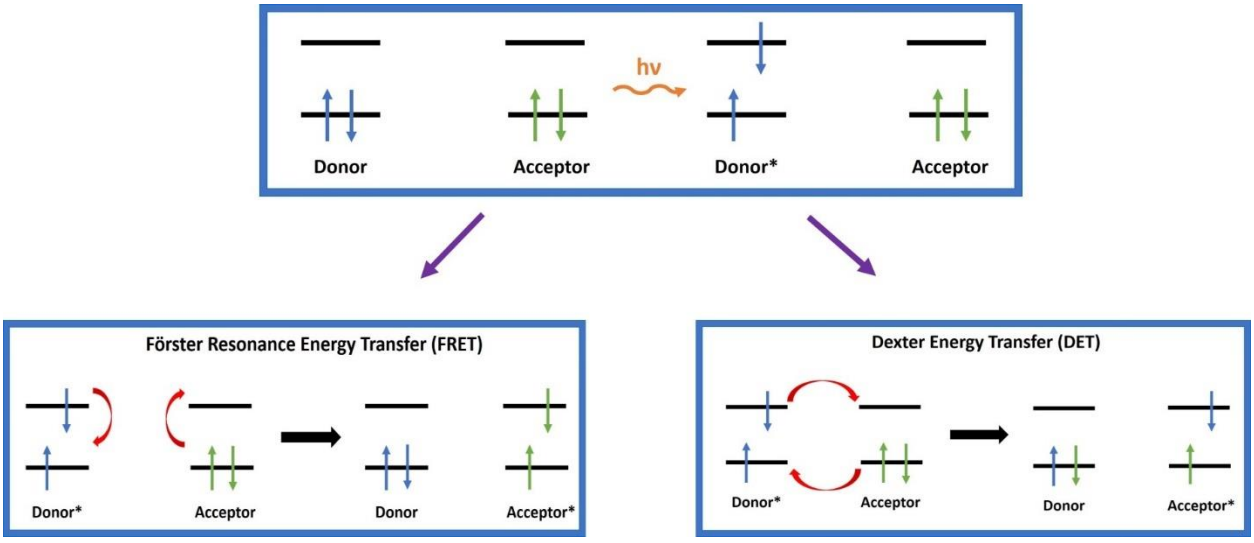

Figure 1. Illustration depicts Förster resonance energy transfer (FRET) and Dexter energy transfer (DET) that can occur between donor and acceptor pairs. The top image shows the photoexcitation of a ground state

donor resulting in either FRET or DET to an acceptor molecule that is in the ground state. The bottom schemes illustrate energy transfer via electronic transitions following FRET or DET leading to the creation of a ground state donor and an excited state acceptor. Adapted with permission from ref. 49. Copyright 2016 Royal Society of Chemistry.

Equation 4 shows the rate constant of DET (k_{DET}) and demonstrates how there is an exponential decay between the donor and acceptor at distances longer than 1 nm.

$$k_{DET} = KJe^{\left(\frac{-2R_{DA}}{L}\right)} \quad (4)$$

In the equation shown above, K is defined as the experimental factor, J is the overlap integral, R_{DA} is the donor-acceptor distance, and L is the sum of the van der Waals radii for the donor and acceptor molecules. For the exchange of an electron to occur within a donor/acceptor system, the wave functions of the separate components need to overlap. Hence, DET strongly depends on the close association between the donor and acceptor molecules at distances around 1 nm. In other words, the conduction band of the inorganic, semiconducting nanocomponent must interact with the LUMO of the organic molecule for electron exchange to occur via the Dexter mechanism in hybrid assemblies. Due to the short distance between donor and acceptor pairs, DET-based studies often concentrate on QDs coupled to small molecular systems, such as polymers or dyes, that result in either a quenching or enhancement in QD photoluminescence. This quenching or enhancement of the QD emission can be monitored using steady-state and time-resolved photoluminescence, in addition to femtosecond transient absorption spectroscopy.[50] The close coupling (~1 nm) between the donor and acceptor molecules via orbital interactions results in faster timescales observed for DET than FRET. Thus, the two mechanisms can be differentiated by examining the spectra and kinetics traces from transient absorption (TA) spectroscopy. The efficiency of either DET or FRET was found to be dependent upon the size of the QD which in turn determined both the distance

between the donor and acceptor.[17, 50] Not only has QD size been paramount in controlling the donor/acceptor spacing in these hybrid assemblies, ligands functionalized on the QD surface have also been reported to impact the rate of Dexter-like energy transfer in such systems.[51] In the following section, we further delineate on the process of triplet-triplet energy transfer (TTET) via the Dexter mechanism.

2.4 Triplet-Triplet Energy Transfer Mediated by Quantum Dots

One recent exciting application of QDs is the coupling of excitons in QDs and the triplet excited states of organic molecules via triplet-triplet energy transfer (TTET). Molecular triplet excited states are characterized by two electrons with parallel spins, which have long lifetimes of micro, milli, or even seconds. The long lifetime allows them to transfer electrons to facilitate many photochemical reactions. However, these triplet states are optically forbidden and cannot be directly photoexcited from the molecular ground state. Hence, a photosensitizer is desired in order to absorb a photon into a singlet state and convert the energy into a triplet state.

Emerging examples of photosensitizers include metal-organic complexes or semiconducting QDs. When metal-organic complexes are utilized as photosensitizers, intersystem crossing enables energy transfer from singlet to triplet states. However, high exchange splitting between the singlet and triplet states of this photosensitizer generates a significant amount of energy loss.[52] On the other hand, there is minimal energy loss when QDs are used as photosensitizers to interconvert a singlet to triplet state. Strong spin-orbit coupling in the QD leads to an exciton that experiences an accelerated spin dephasing and exhibits both singlet and triplet character.[53] As shown in Figure 2, a spin-allowed energy transfer is possible between the “triplet” QD exciton and the triplet state of the molecular acceptor.[54] The creation of two molecular triplet states in the acceptor can result in the termination of these two states yielding a higher energy

molecular singlet state. The termination of these two triplet states is referred to as triplet-triplet annihilation resulting in the emission of a higher energy photon. By modifying the molecular structure of the acceptor or QD size or shape, it is possible to modulate TTET to generate either an upconversion or a downconversion in photons, which will be further discussed in the following sub-sections. The ability to up- or down- convert photons is highly advantageous in optoelectronic applications.[55, 56]

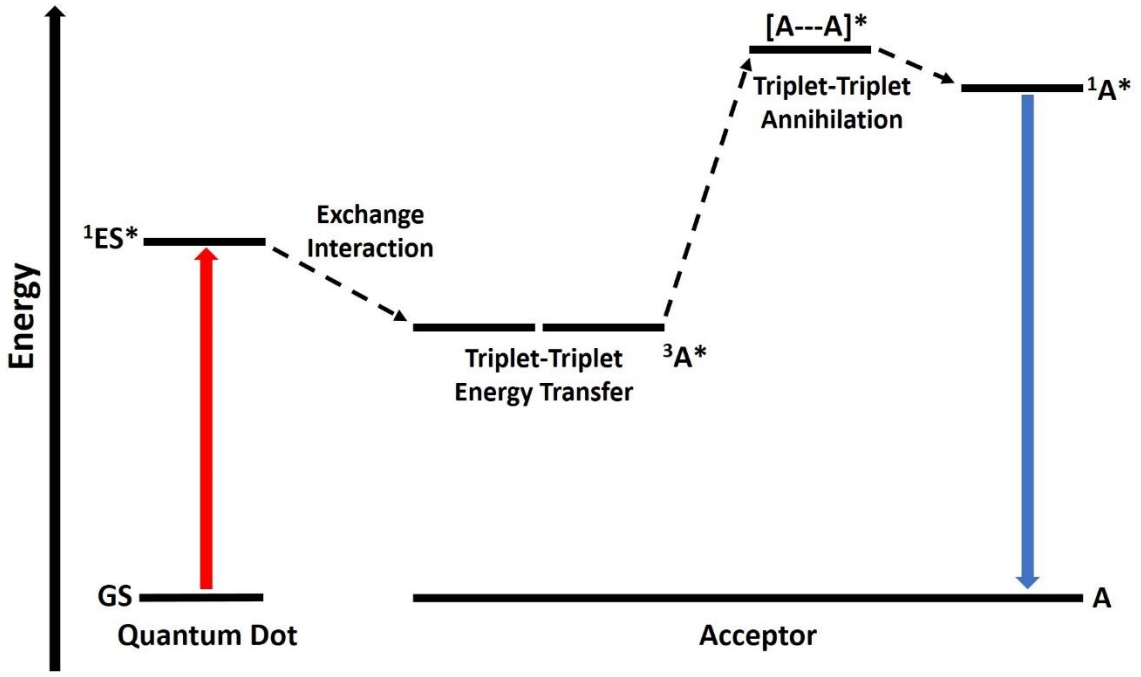

Figure 2. Diagram depicts the triplet-triplet annihilation process that occurs between a QD photosensitizer and an acceptor molecule leading to photon upconversion. Photoexcitation of the QD sensitizer leads to excitation from the ground state (GS) to an excited singlet state (^{1}ES*) in the QD. As a result of strong spin-orbit coupling in the QD, the exciton experiences spin dephasing and displays both singlet and triplet character. A spin-allowed energy transfer is possible between the "triplet" QD exciton and a triplet state of the acceptor (^{3}A*). The excited triplet states of the acceptor can then terminate into a higher energy singlet state (^{1}A*) via triplet-triplet annihilation ([A---A]*), resulting in the emission of a photon with higher energy than the incident photon. Adapted with permission from ref. 54. Copyright 2010 Elsevier.

3. OPTICAL FEATURES OF HYBRID QUANTUM DOT/SMALL MOLECULAR SYSTEMS

Hybrid nanosystems composed of QD and small molecules have been explored for energy-related device applications (i.e., solar cells, light-emitting diodes, etc.) due to the tunability in their optoelectronic properties by joining QDs with small moleulces.[13, 57-60] Specifically, there has been a growing interest to study the competing energy transfer processes such as FRET and DET in these systems which influence the optical properties of the heteroassemblies. In this section, we focus our attention on the infrared (IR) dye, squaraine, and J-aggregates coupled to QDs.

3.1 Förster Resonance Energy Transfer vs. Dexter Energy Transfer in QD/Squaraine Coupled Systems

Although QDs possess a multitude of favorable properties for solar light harvesting applications,[7, 61, 62] one major drawback of the commonly used CdSe/ZnS (core/shell) QDs is that they do not absorb light in the IR region of the electromagnetic spectrum. Although advancements have been made in the fabrication of colloidal QDs that can absorb and emit light in the IR region,[63-66] it is convenient to broaden the absorption of the most well-developed CdSe-based QDs by coupling them with IR-absorbing dyes.[67, 68] Such examples have been demonstrated by Choi and coworkers, in which a dye from the squaraine (SQSH) family was covalently linked to CdSe QDs and titanium dioxide (TiO_2) nanoparticles.[50, 59, 68]

Interest has been concentrated on squaraine dyes due to their strong absorption in the near-infrared (NIR) region of the electromagnetic spectrum and high molar extinction coefficients.[69, 70] The SQSH molecule (molecular structure shown in Figure 3A) played a dual role in these hybrid systems, in which the dye acted as a bridge between the QDs and TiO_2 film and as a NIR absorber.

A stepwise synthesis was executed to create the NIR SQSH linker with a HS-R-COOH configuration that displayed similar functionalities to 3-mercaptopropionic acid (3-MPA).[59] The SQSH linker connected CdSe QDs to a TiO_2 film for the potential use of this hybrid assembly to be employed in a solar cell design. In this study, the SQSH molecule first acted as a FRET acceptor to the CdSe QD and then as an electron injector into the TiO_2 film. The results indicated a successful energy/electron transfer from the CdSe QDs to the TiO_2 film mediated by the SQSH linker. Moreover, the power conversion efficiency was recorded to be 3.65% for the hybrid solar cell design. Hoffman and coworkers expanded upon these previous findings to gain further insight into the energy transfer processes between QDs and the SQSH linker. In a later work, equimolar amounts of QDs and the SQSH molecules were mixed together resulting in a broadened absorption of the assembled system from the visible to the NIR region of the electromagnetic spectrum. Furthermore, upon photoexcitation at 440 nm, a decrease in the QD photoluminescence, concomitant with an increase in the SQSH emission, was observed (Figure 3C) due to FRET from the QDs to SQSH.

In addition to FRET, the possibility of DET in the QD/SQSH system was also investigated.[50] Steady-state photoluminescence and femtosecond TA spectroscopy were utilized to differentiate between the FRET and DET mechanisms. Efforts were devoted to understanding how DET competes with FRET and how the QD size determines the occurrence of either DET or FRET. The diameters of the QDs studied ranged from 3 – 5 nm, and the SQSH dye was covalently attached to the QD by thiol linkages (Figure 3A). The results demonstrated that the QD diameter did dictate which energy transfer mechanism would dominate. The TA spectroscopy experiments revealed that energy transfer on the ultrafast timescale decreased upon increasing the diameter of the QD donor. It was concluded that the ultrafast photoluminescence quenching (~200 ps) was the

result of energy transfer via DET, whereas slower photoluminescence quenching (~1 ns) was due to FRET for QDs that had a ~3 nm diameter. As illustrated in the energy level diagrams of Figure 4B, DET was the principal energy transfer pathway for smaller sized QD (i.e., 2.7 and 2.9 nm) as a result of greater orbital interactions between the individual QD and SQSH dye. However, as the diameter of the QD increased, DET was less influential due to smaller energy level overlap between the conduction band of the QD and the LUMO of SQSH. Nevertheless, the prospect of DET as a leading energy transfer mechanism over FRET should not be overlooked, in particular for light-harvesting systems, and future studies are needed to corroborate this idea.[71]

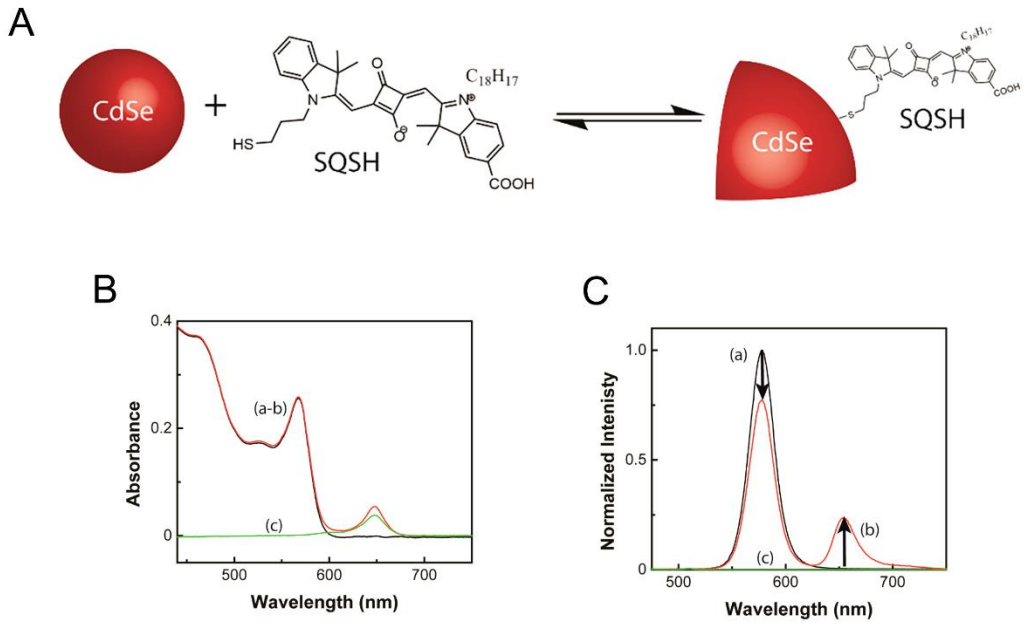

Figure 3. (A) Schematic illustrating the sulfur from the thiol group of the squaraine (SQSH) dye binding to the CdSe QD. **(B)** Absorbance and **(C)** Photoluminescence spectra of (a) 4.3 nm CdSe QDs, (b) Mixture of 4.3 nm CdSe QDs with SQSH in equimolar amounts, and (c) SQSH in toluene. Reprinted with permission from ref. 50. Copyright 2014 American Chemical Society.

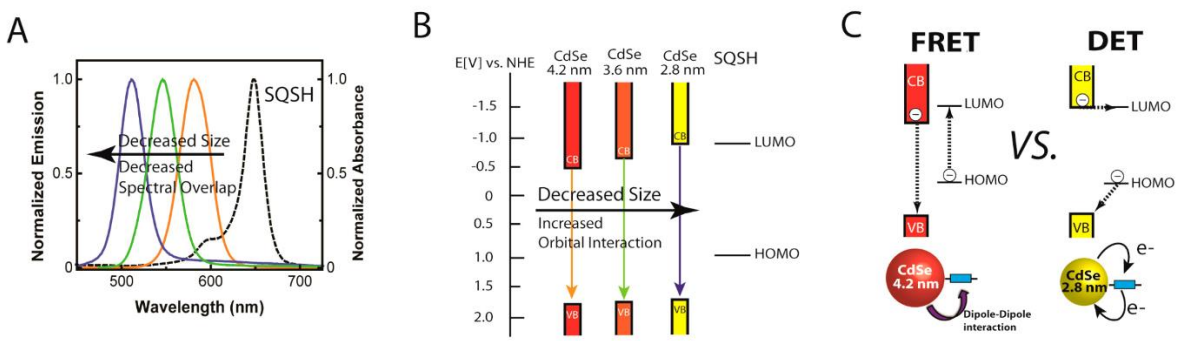

Figure 4. (A) Normalized absorption spectrum of squaraine (SQSH) dye and normalized emission spectra of different size CdSe QDs. **(B)** Energy level diagram of QDs and SQSH dye. As the diameter of the QD is decreased, there is greater energy band alignment between the QD and HOMO and LUMO of SQSH, leading to Dexter energy transfer (DET) dominating the system. **(C)** Diagram demonstrates the difference between FRET and DET in the QD/SQSH system. Reprinted with permission from ref. 50. Copyright 2014 American Chemical Society.

3.2 Enhanced Optical Features and Energy Transfer in QD/J-aggregate Coupled Systems

J-aggregates of dyes are ordered supramolecular systems that exhibit interesting optical properties for photoelectric applications.[72-74] These unique optical features include a large oscillator strength, small Stokes shift, and sharply narrow absorption band. Additionally, photoexcitation of J-aggregate systems yields chromophore coupling and the delocalization of excitation energy within the aggregates, which has been extensively studied in the literature.[75-79] Due to the impressive optical features of J-aggregates, many have coupled these structures with QDs to investigate the viability of energy transfer in a hybrid QD/J-aggregate system. When J-aggregates are conjugated to QDs, they can act as antennas to strongly absorb light in a specific wavelength range due to their large absorption cross-sections. The energy can then be transferred to QDs resulting in light emission in low-intensity or diffuse lighting. Therefore, such hybrid QD/J-aggregate system will have higher light utilization efficiency than isolated QDs. Earlier

studies conducted by Walker *et al.* integrated thiacyanine J-aggregates with CdSe/ZnCdS QDs both in solution and on spin-casted films.[80, 81] These studies highlighted an enhanced light absorption and an increase in the QD photoluminescence as shown in Figure 5. Furthermore, high energy transfer efficiencies (~90%) were reported from both works, demonstrating how thiacyanine J-aggregates act as effective light harvesting antennas in these hybrid assemblies.

More recent works have investigated the utilization of J-aggregates to enhance the NIR absorption of PbS QDs. There has been a burgeoning interest in Pb-based QDs due to the strong absorption and high emission of Pb-based QDs in the NIR region of the electromagnetic spectrum, leading to the possibility of Pb-based QDs in solar applications. As previously explained, QDs possess many unique photophysical characteristics. One such intriguing photophysical property of QDs, in particular of PbS QDs, is the capability of QDs to downconvert incident photons to many lower-energy photons, resulting in photon downconversion.[82] The process of photon downconversion is highly advantageous for signal or photocurrent amplification in QD-based sensors or photovoltaics, respectively. However, fast Auger recombination of excitons in the QDs competes with photon downconversion and makes it challenging to make use of the NIR excitons. To circumvent the possibility of Auger recombination in QD systems, molecular J-aggregates have been incorporated into QD assemblies for fast extraction of NIR excitons from the PbS QDs to the J-aggregates via FRET. Wang and coworkers successfully demonstrated sub-nanosecond energy transfer from PbS QD donors to the J-aggregate cyanine dye acceptor, IR-140-Cy^+, in colloidal solutions.[83] The fastest exciton extraction was recorded to be ~90 ps and found to be potentially competitive with the Auger recombination process. To expand upon their QD/J-aggregate work, Wang *et al.* explored the possibility of a J-aggregate acting as a molecular bridge between the donor and acceptor QDs to further accelerate the transfer of NIR excitons.[84]

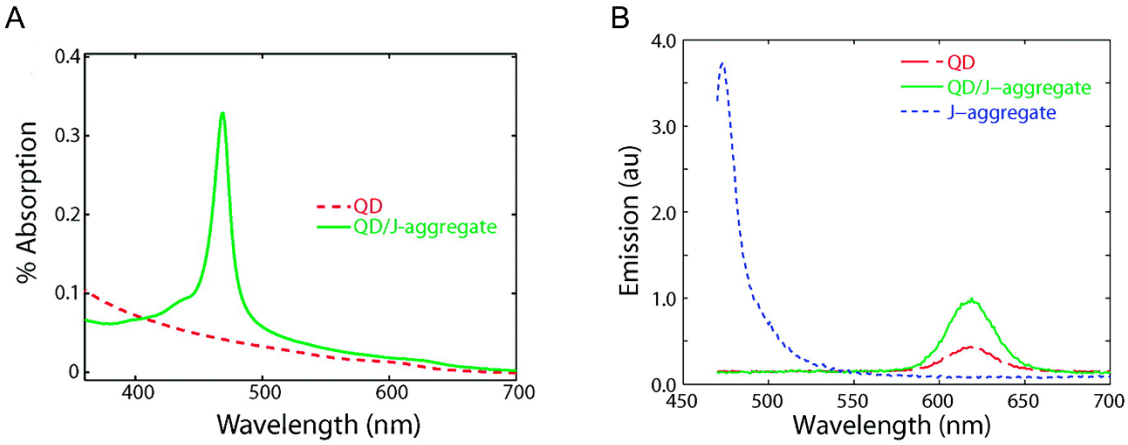

Figure 5. (A) An enhanced absorption of CdSe/ZnCdS QDs is observed when the QD is coupled to J-aggregates. **(B)** The coupling of QDs with J-aggregates results in an increase in the QD emission. Reprinted with permission from ref. 80. Copyright 2010 American Chemical Society.

Their work published in 2017 demonstrated the potential of relayed energy transfer in composite films, in which a J-aggregate layer of the cyanine dye, IR-140-Cy$^-$, was sandwiched between layers of PbS/CdS QDs that acted as donor (DQD) and acceptor (AQD) QDs within the system as shown in Figure 6. The donor and acceptor QDs were rendered positively charged by encapsulating the QDs in the molecule, 2-aminoethanethiol (AET). A layer by layer protocol (LbL) was implemented to design the QD/J-aggregate composite film. The initial step of the LbL procedure entailed coating the glass substrate with solutions of poly(diallyldimethylammonium) chloride (PDDA) and poly(sodium 4-styrenesulfonate) (PSS). Subsequent steps of the LbL method involved immersing the substrate in a solution of the DQDs, an IR-140-Cy$^-$ solution, and a solution of AQDs. Transient absorption (TA) spectroscopy was utilized to monitor the energy transfer within the QD/J-aggregate/QD film. Unlike previous PbS QD studies which reported energy transfer within a few nanoseconds between donor and acceptor QDs,[85-88] a sub-nanosecond transfer of NIR excitons was achieved from the QD donor to QD acceptor, because of the J-aggregate

linker resulting in a relayed FRET assembly. Specifically, a 20-fold increase in the energy transfer efficiency was observed for the QD/J-aggregate/QD assembly compared to isolated QD systems. Accelerating the extraction of excitons from QDs is highly desired for applications that are contingent on ultrafast charge separation for optimal device performance.

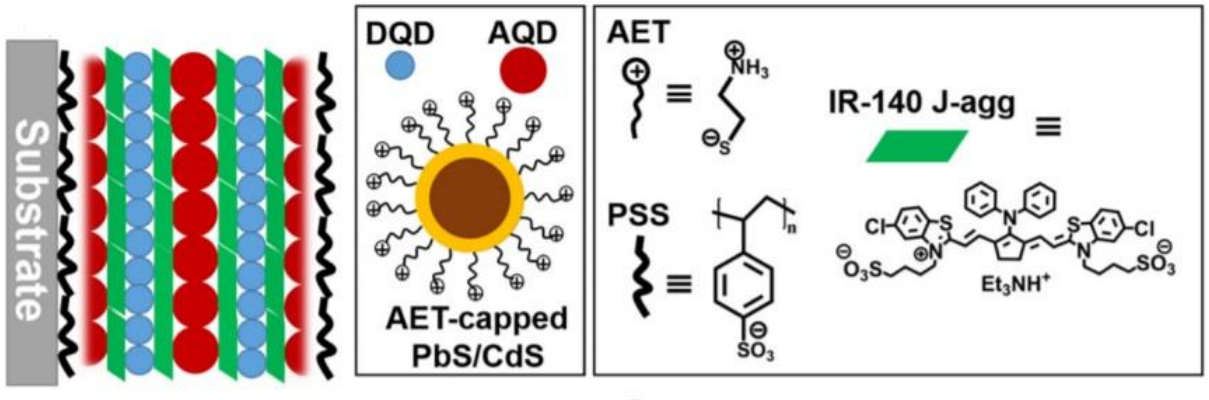

Figure 6. Scheme demonstrates the sandwiched structure of the QD/J-aggregate/QD film. Donor (DQD) and acceptor (AQD) PbS/CdS QDs were first coated in 2-aminoethanethiol (AET) rendering the QDs with a positively charged surface. The glass substrate was initially immersed in the polymers, poly(diallyldimethylammonium) chloride (PDDA) and poly(sodium 4-styrenesulfonate) (PSS). The films were created via a layer by layer (LbL) method in which the positively charged PbS/CdS QDs electrostatically interacted with the negatively charged J-aggregate of the cyanine dye, IR-140-Cy. Findings demonstrated an acceleration in NIR exciton movement from DQD to AQD via the J-aggregate bridge compared to previous works focused on direct energy transfer between QDs. Reprinted with permission from ref. 84. Copyright 2017 American Chemical Society.

Others have also demonstrated the ability of J-aggregates to act as light-harvesting antennas in QD/J-aggregate assemblies. One study conducted by Freyria *et al.* explored the interaction between self-assembled molecular J-aggregates from the cyanine dye, C8S3, that were mixed in a colloidal solution of IR-emitting PbS QDs.[89] The QD/J-aggregate assemblies were also

prepared in solid matrices in the same work. Despite no direct conjugation between the J-aggregates to QDs, an enhancement was still observed in the QD emission for both liquid and solid media. This enhancement in QD emission was attributed to efficient funneling of excitons by the J-aggregates, resulting in the observed "antenna" effect.

3.3 Triplet-Triplet Energy Transfer via the Dexter Mechanism in Quantum Dot/Molecular Assemblies

Recent work performed on TTET in QDs coupled to various molecules in the acene family highlights the prominence of the Dexter mechanism.[90, 91] One such study conducted by Tabachnyk *et al.*[90] demonstrated TTET from the molecule, pentacene, to PbSe QDs in organic semiconducting films. The molecular triplet excitons of pentacene were produced upon singlet exciton fission and transferred to PbSe QDs at the bilayer interface of the film. The transfer of the triplet excitons of pentacene to QDs was probed using ultrafast absorption spectroscopy and was discovered to occur on a sub-picosecond timescale. Moreover, Tabachnyk and coworkers investigated the effect of tuning the band gap of the PbSe QD on TTET and found that the most efficient TTET occurred when the QD band gap was close in energy to the triplet energy of pentacene. The work conducted by Tabachnyk *et al.* illuminates on the necessity of orbital overlap between the donor and acceptor for efficient TTET.

Alternative studies have explored the roles of visible and IR-emitting QDs as triplet sensitizers in molecular QD systems. As mentioned above, triplet excited states of organic molecules are desired in many photochemical reactions, but the formation of the triplet excited state is often inefficient because direct excitation from a singlet ground state to a triplet state is forbidden by the spin-selection rules. The TTET process from QDs to molecular triplet states provides an efficient alternative to generate molecular triplets. Due to the ill-defined spin character

of QDs,[92] the triplet exciton energy of QDs cannot be directly transferred to the molecular triplets. The pioneering work by the Castellano group[93] demonstrated that triplet excitons from QDs can be extracted by two types of triplet acceptor molecules that are anchored onto the QD surface. The TTET mechanism in this system was evident by the correlation between the decay of the exciton in the CdSe QDs and the growth of the triplet state of the acceptor molecule using ultrafast TA spectroscopy. The quantum efficiency of TTET in the system was reported to be higher than 90%.

Nuanced factors can also play a critical role in mediating the rate of TTET in hybrid QD-molecular systems. For example, the impact of ligand length on TTET was investigated by Nienhaus and coworkers,[51] in which carboxylic acid ligands acted as spacers between PbS QDs and rubrene molecules in a bilayered film. The rubrene layer was doped with the emitter molecule, dibenzotetraphenylperiflanthene (DBP), to enhance the emission of the rubrene film. Photoexcitation of the QDs sensitized the triplets in rubrene, resulting in triplet-triplet annihilation and the creation of singlet states in the rubrene layer. They demonstrated that the termination of these two triplets yielded photon upconversion in their solid-state structure and reported an increase in the upconversion efficiency compared to previous studies.[94] By decreasing the length of the ligands passivated onto the QD surface, Nienhaus *et al.* discovered that the rate of triplet energy transfer (k_{TET}) was dependent upon the effective dielectric constant of the bilayered structure. As shown in Figure 7, it was found that the TET time ($\tau_{TET}, k_{TET} = \frac{1}{\tau_{TET}}$) asymptotes at $\tau_{TET} \approx 100$ ns when the QD shell thickness was ≤ 10 Å. Hence, the extracted TET rate k_{TET} for QDs functionalized with shorter ligands was slower than what was previously reported in the literature.[90, 93] Furthermore, a direct exponential relation was expected between k_{TET} and the donor-acceptor spacing (L_C) as can be determined using Equation 5.

$$k_{TET} \sim |V|^2 e^{-2L_C/L_{TET}} \quad (5)$$

Equation 5 demonstrates how the triplet energy transfer rate (k_{TET}) is related to the electronic coupling between the donor and acceptor (*V*), in addition to the ligand shell thickness (L_C) and the characteristic TET length (L_{TET}). Tuning the ligand length not only impacted the spacing between neighboring QDs and the QD/rubrene film interface, but also increased the number of QDs in the QD monolayer, resulting in an increase in the dielectric screening of the excitons. The combination of the high dielectric constant (ε) of PbS QDs[95] with the lower dielectric constants of the ligands yielded a greater change in the effective medium dielectric constant. Since the electronic coupling constant (*V*) in Equation 5 is inversely proportional to the medium dielectric constant $\left(V \sim \frac{1}{\varepsilon}\right)$,[48, 96] this would mean that k_{TET} is also inversely related to the dielectric constant of the medium. Thus, the slower rate of TTET (k_{TET}) was attributed to an increase in the dielectric constant of the film as a result of a greater volume of PbS QDs (shell thickness ≤ 10 Å) in the QD layer. In order to obtain the expected exponential relationship between k_{TET} and L_C (Equation 5), a separate equation was used to normalize k_{TET} so that it was independent of the effective medium dielectric constants. By normalizing k_{TET}, the anticipated exponential trend between k_{TET} and the donor-acceptor spacing (L_C) was achieved in this study.

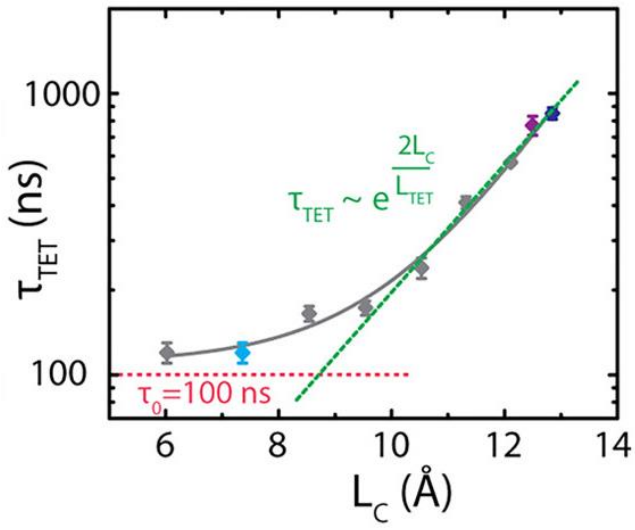

Figure 7. The triplet energy transfer times (τ_{TET}) plotted as a function of the donor-acceptor spacing (L_C) between the PbS QDs and rubrene molecules. The aliphatic ligands functionalized on the QD surface were varied from longer ligands (i.e., oleic acid, OA, and stearic acid, 18C) to shorter ligands (i.e., hexanoic acid, 6C). "18C" and "6C" refers to the number of carbon atoms in the ligand chains. The green dashed line denotes the anticipated exponential relationship between that of τ_{TET} and the ligand shell thickness (L_C) and characteristic TET length (L_{TET}). The gray line represents the experimental discrepancy from the theoretical result, in which the τ_{TET} saturates at ~100 ns when the QD shell thickness is ≤ 10 Å. Reprinted with permission from ref. 51. Copyright 2017 American Chemical Society.

A parallel study conducted by Bender *et al.*[97] concentrated on how the creation of surface sites upon the attachment of TIPS-pentacene (2-CP) on PbS QDs impacted TTET in QD-acene heterostructures. Upon absorption of IR photons, excitons generated in the PbS QDs were transferred to the covalently linked molecules, resulting in the creation of triplet excitons. The formation of these triplet excitons was monitored with TA spectroscopy as shown in the TA spectra in Figures 8A and 8B. Spectral signatures illustrated the generation of triplet excitons by a positive absorbance band at ~525 nm as previously shown in the literature.[98, 99] Figure 8A demonstrates the progression of the 2-CP:PbS QD TA spectrum at increasing pump-probe time delays. The

photobleached feature at 715 nm decays to baseline, while an induced absorption band emerges at ~535 nm over longer time delays. Moreover, additional photobleached signals are apparent at ~607 and ~657 nm. Comparisons were then made between the 2-CP triplet state spectrum obtained from photosensitization measurements and the extracted TA spectral feature at ~535 nm taken from the 2-CP:PbS QD sample (Figure 8B). It was determined that excitation of the PbS QDs yielded 2-CP triplet excitons as evidenced by the good agreement between the two TA spectra. Based on their findings, Bender *et al.* concluded that these triplet excitons were created via a kinetic intermediate that was comprised of a concerted hole and electron transfer event from the QDs to 2-CP molecules. The surface states formed due to the covalent attachment of 2-CP localized excitations within the heteroassembly, ultimately slowing the TTET process. In order to expedite the production of triplet excitons, Bender and coworkers suggested that improvements must be made to QD surface passivation methods to eliminate surface states from mediating TTET.

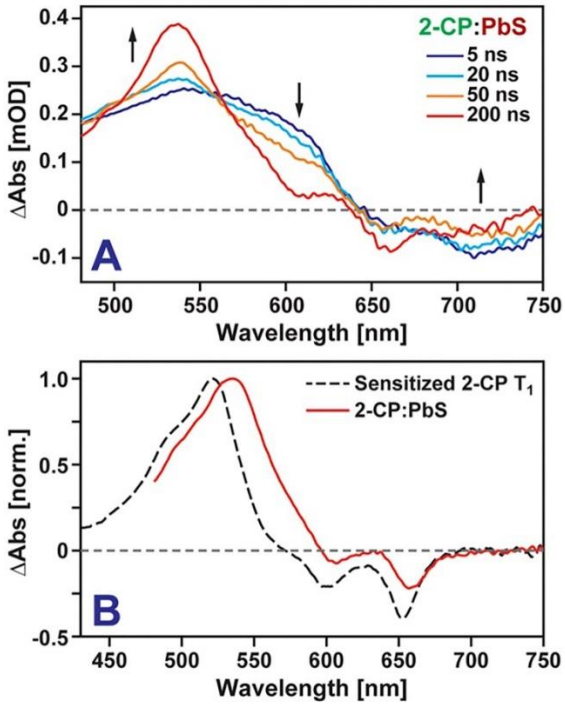

Figure 8. (A) Transient absorption (TA) spectra collected at different pump-probe time delays for TIPS-pentacene (2-CP) and PbS QD samples. Arrows indicate the formation and decay of absorption bands. **(B)** The black dashed line represents the TA spectrum of the 2-CP triplet excitons, which was obtained from solution phase sensitization studies. The red solid line signifies an extracted spectral feature from the TA spectrum of 2-CP:PbS QDs taken at ~200 ns. Since the lineshapes appear almost identical between the two spectra, it was concluded that excitation of the 2-CP:PbS QD system generated 2-CP triplet excitons. Reprinted with permission from ref. 97. Copyright 2018 American Chemical Society.

4. QUANUTM DOT AS ENERGY DONOR OR ACCEPTOR IN HYBRID BIOLOGICAL SYSTEMS FOR ENERGY-RELATED APPLICATIONS

Complexed nanosystems have been developed that mimic similar functions to those found in nature. Both plants and bacteria possess light harvesting components, such as chlorophylls and carotenoids, that have been conjugated with QDs to create intricate nanosystems for solar energy conversion. Compared to historically used organic fluorophores, QDs are capable of capturing

light over a wider spectral range, leading to an overall enhancement in the light energy conversion of a hybrid QD assembly that would be ideal for an artificial antenna system. The focus of this section concentrates on the role of QD as either a donor or acceptor in advanced hybrid structures. These systems incorporate biological materials ranging from light harvesting complexes (i.e., LHCII) to the photochromic protein, bacteriorhodopsin (BR).

4.1 Light Harvesting Complex II as Potential Energy Donor to QD in Coupled System

Light harvesting complex II (LHCII) is the most abundant light harvesting system found on earth. This complex is comprised of both proteins and chlorophyll a/b molecules that are affixed to the thylakoid membrane of higher plants and are associated with photosystem II. Moreover, LHCII demonstrates high photostability due to the carotenoids in the complex that prevent oxidation of the chlorophylls. Upon photoexcitation, energy is transferred from the core pigment (chlorophyll a) and antenna pigments (chlorophyll b, xanthophylls, and carotenoids) to the reaction center of the photosystem leading to photosynthesis.

Due to the broad range of light absorption by QDs, studies have focused on QDs as the donor molecule to enhance the absorption of the light harvesting complexes.[9, 25, 100] However, work conducted by Werwie *et al.*[101] demonstrated that the biological component of a hybrid system could also serve as an energy donor. In this study, CdTe/CdSe/ZnS QDs were electrostatically bound to the light harvesting complex, LHCII. Figure 9A displays the absorption features after assembling LHCII with QDs, that are different from the individual absorption spectra. To increase the nonradiative energy transfer efficiency between LHCII and QDs, QDs with an absorption spectrum that overlapped with the LHCII emission spectrum were chosen for this system. As illustrated in Figure 9B, there is a faster photoluminescence decay of the LHCII donor when it was coupled to the QDs.

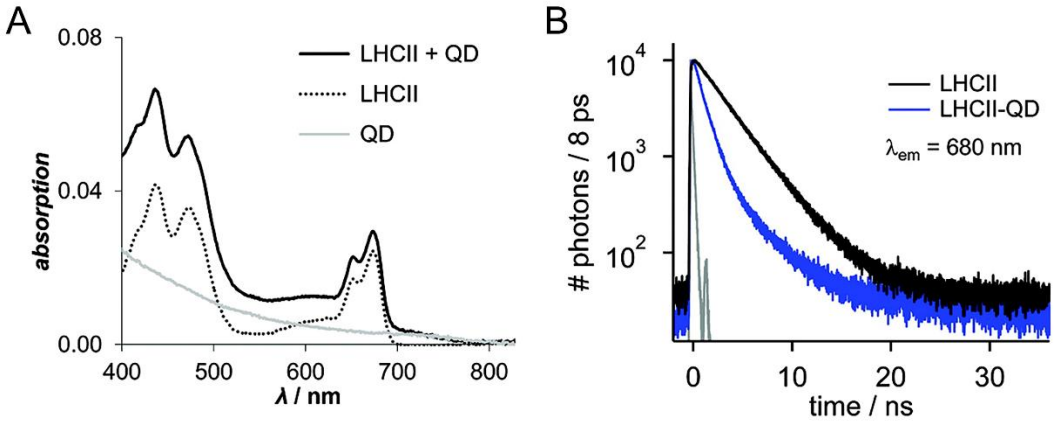

Figure 9. (A) Absorption spectra of light harvesting complex II (LHCII) with and without QDs, respectively. **(B)** Photoluminescence decays of LHCII coupled to and without QDs. Reprinted with permission from ref. 101. Copyright 2012 American Chemical Society.

Energy transfer via the FRET mechanism was quantitatively determined by calculating the areas under the donor (A_q) and acceptor (A_s) emission profiles. If a system displays FRET-like energy transfer, the decreased area under the quenched donor emission would be equivalent to the increased area under the sensitized emission spectrum of the acceptor. Thus, a ratiometric determination between $\frac{A_s}{A_q}$ would be close to unity for a system that exhibits FRET. In this case, the calculated ratio of $\frac{A_s}{A_q}$ for the QD/LHCII assembly was determined to be 1.1 indicative of a FRET-like energy transfer.

An additional experiment was conducted that focused on enhancing the absorption cross-section of the hybrid complex in the entire visible region. Previous work has shown the existence of a "green gap" in the visible region of the chlorophyll absorption spectrum.[102] To circumvent this issue, dyes (i.e., the Alexa Fluor dyes) were adhered to LHCII to increase the light absorption of the complex.[102-104] The hybrid LHCII/dye/QD system had a broader absorption range in the

entire visible region, showing its potential as a biomimetic light harvester for photovoltaic applications. However, further work is needed to improve upon the photostability of the hybrid complex before implementation of this system in commercial devices.

4.2 Quantum Dot Energy Donor Demonstrates Enhanced Biological Function of Reaction Centers in Purple Bacteria

Unlike the previous study which focused on the reaction center of photosystem II in green plants, other works have concentrated on QDs as the donor responsible for an enhancement in exciton generation in bacterial systems.[25, 71, 105] In 2010, Nabiev *et al.*[106] demonstrated a three-fold increase in exciton generation as a result of energy transfer from CdTe QDs to the reaction centers (RCs) in the well-studied purple bacteria, *Rhodobacter sphaeroides* (*Rb. sphaeroides*). Figure 10A illustrates integral components of the RC extracted from the purple bacteria in the heteroassembly. The RC is comprised of two building blocks, one of which is an active site that is responsible for electron-hole separation and electron transfer. Both the active and inactive branches have one bacteriochlorophyll (B_A or B_B), one bacteriopheophytin (H_A or H_B), and one quinone (Q_A or Q_B) in each branch as shown in Figure 10A. A dimer of bacteriochlorophylls acts as a bridge between the two sites and is called P870 (Figure 10A). Initial light excitation of the RC results in electron-hole separation at P870 that channels an electron toward the quinone in the active branch. As shown in Figure 10B, the bacteriochlorophyll pair of P870 displays an emission peak at ~910 nm.

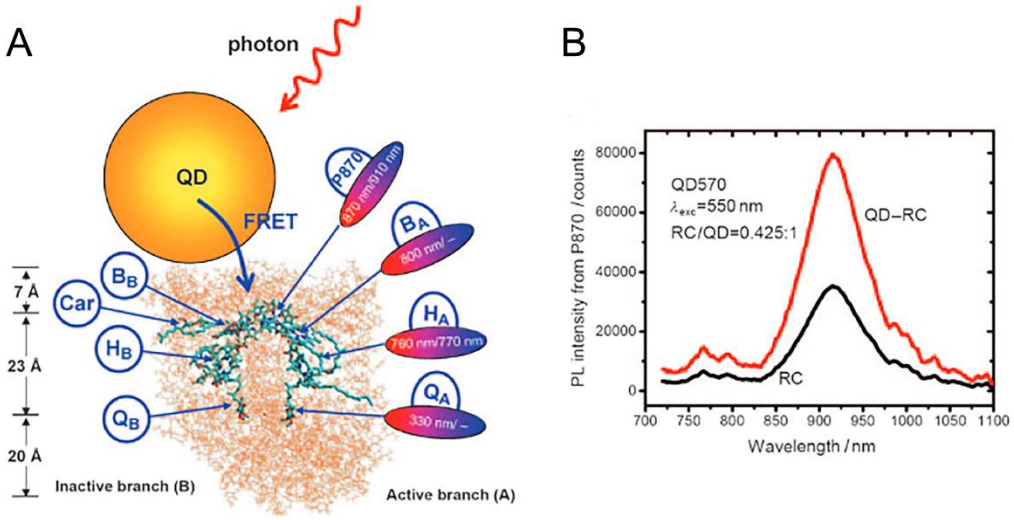

Figure 10. (A) A simplified illustration highlights the structure of the reaction center (RC) from *Rhodobacter sphaeroides* (*Rb. sphaeroides*) coupled to a QD. The reaction center is divided into an active (A) and inactive (B) branch. Electron-hole separation and transmembrane electron transfer occur at the active branch. The active and inactive branches are each comprised of one quinone (Q_A or Q_B), one bacteriochlorophyll (BChl, B_A or B_B), and one bacteriopheophytin (H_A or H_B). A dimer of BChl molecules (P870) acts as a bridge between the two branches and is responsible for charge separation at the active branch. The carotenoid of *Rb. sphaeroides* is located in the inactive branch and is labeled "Car" in the figure. **(B)** An enhancement in the emission of the bacteriochlorophyll dimer (P870) is apparent after coupling with QD nanocrystals. Reprinted with permission from ref. 106. Copyright 2010 Angewandte Chemie.

Similar to the QD/LHCII study, the hybrid QD/RC assemblies were formed by electrostatic interactions. Unlike the previous mentioned LHCII work, here the QDs act as artificial light harvesting antennas that transfer energy to the RC acceptors. The QD photoluminescence was overlapped with the absorption spectra of the RC chromophores in order to achieve energy transfer via FRET within the assembly. Photoexcitation of the hybrid structure resulted in an enhancement in the emission of the RC due to an increase in the number of excitons created at the RC site.

Förster-type energy transfer was also confirmed by both time-resolved and steady-state photoluminescence experiments conducted on the QD/RC moieties at different molar ratios. The greatest photoluminescence enhancements were recorded for the smallest RC/QD molar ratios as a result of more QDs coupled to one RC site. This study by Nabiev and coworkers was one of the first to prove an efficient energy transfer between inorganic nanocrystals, acting as artificial light harvesters, and a sophisticated photosynthetic complex.[106]

4.3 Tunability of Bacteriorhodopsin Photocycle Kinetics due to a QD Energy Donor

Work conducted in our own group[107] has explored the interaction between colloidal QDs and the photoactive protein, bacteriorhodopsin (BR). Upon light absorption of BR, a well-characterized photocycle is initiated that leads to a net translocation of a proton from the cytoplasmic surface to the extracellular domain of the lipid bilayer membrane that contains BR.[108, 109] The primary photointermediate of this photocycle is often referred to as the **K** photostate (λ_{max} = 590 nm) and is characterized by a strained 13-*cis* conformation of the light absorbing chromophore, retinal, which drives all subsequent photocycle reactions in BR.[110-112] Following the generation of **K**, the protein decays through the spectrally distinct photointermediates—the **L**, **M**, **N**, and **O** states—before returning to the resting state (**bR**).[113]

In our own study, we have investigated how the interaction between QDs and BR in solution enables the direct modulation of the lifetime of the photocycle. Although numerous research groups[114-116] have studied the influence of BR on the emission properties of the QDs, there have been limited investigations that explore how QDs impact the kinetics of the BR photocycle. For our work, CdSe/CdS QDs were added to individual solution samples of the BR mutant, A103C. We selected this mutant to enable the conjugation between the protein and QDs in solution. The **M** and **bR** photointermediates were monitored via time-resolved absorption spectroscopy in the

presence of QDs. The historical importance of the **M** and **bR** photostates stems from the **M**/**bR** pairing being utilized as a photochromic medium in computing systems designed with biological materials.[117] Figure 11 illustrates the time-dependent evolution of the **M** and **bR** photointermediates as shown in two-dimensional heat maps for A103C/QD assemblies at different molar ratios (i.e., 900:1, 500:1, and 300:1). As the relative concentration of QDs increased in solution, the **M** and **bR** decay photointermediate lifetimes were elongated. Meanwhile, photoluminescence quenching of the QDs by BR was also evident from the QD fluorescence lifetime measurements indicative of a nonradiative energy transfer. From our experimental findings, we propose that the fixation of QDs to the protein affects the proton translocation during the photocycle of BR, and the excitonic coupling between BR and QDs leads to modified kinetics of the BR photocycle.

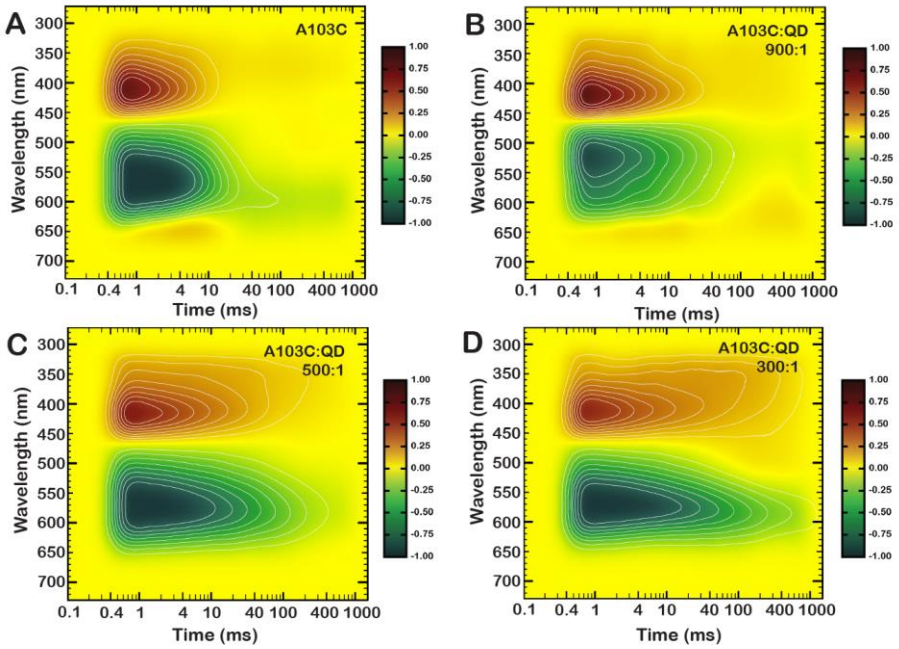

Figure 11. The evolution of the **M** and **bR** photointermediates for each A103C/QD system was followed using two-dimensional heat maps for **(A)** A103C, **(B)** 900:1, **(C)** 500:1, **(D)** 300:1. The heat maps demonstrate elongations in the **M** (410 nm, positive red peak) and **bR** (570 nm, negative green peak)

photointermediates for A103C/QD assemblies, specifically for A103C/QD systems that have high QD concentrations (Panels C and D). Reprinted with permission from ref. 107. Copyright 2019 Springer Nature.

4.4 Higher-Ordered, Self-Assembled Heterostructures Consisting of Stable Protein One and QDs

In our own QD/protein study and others,[30, 107, 118, 119] the hybrid assemblies were created by non-specific or electrostatic interactions between the QD and the protein. Recently, there has been considerable effort by various research groups to produce self-assembled protein systems with control.[118, 120-123] Constructing such complexed systems has proven to be a challenging feat due to the heterogeneity of the protein structure. Nonetheless, there have been multiple works that have proposed several ways to design higher-ordered, self-assembled heterostructures.[124, 125] One protein, in particular, that has been considered for higher-ordered systems is stable protein one (SP1), or the cricoid protein. Stable protein one is a ring-like protein that is comprised of 12 sub-units through hydrophobic interactions. The double-layered, six-membered ring has a negatively charged structure and displays high symmetry. Similar to BR, SP1 exhibits high thermal and chemical stability, which has made the protein ideal for bio-nanotechnology applications.[126, 127] Self-assembled, hybrid systems of SP1 and QDs have been successfully engineered by Miao and coworkers.[128] Varying sizes of CdTe QDs (QD1: 3.3 nm, QD2: 5.8 nm, and QD3: 11.5 nm) were electrostatically assembled onto the SP1 scaffold as illustrated in Figure 12A.

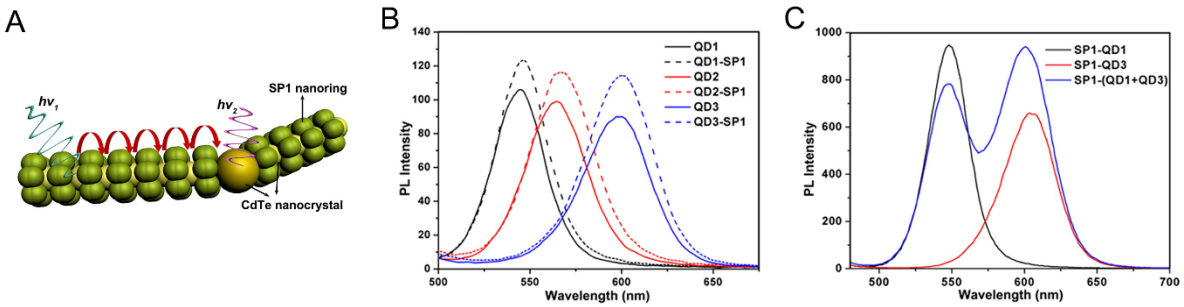

Figure 12. (A) Illustration depicts the self-assembly of the SP1 protein onto different sized QDs and the relayed energy transfer in the system. **(B)** Emission spectra of QD1 (3.3 nm), QD2 (5.8 nm), and QD3 (11.5 nm) and QD/SP1 assemblies. **(C)** Emission spectra of QD1/SP1, QD3/SP1, and a mixture of QD1 and QD3 with SP1. Reprinted with permission from ref. 128. Copyright 2014 American Chemical Society.

The conjugation of QDs with SP1 resulted in an enhancement of the QD emission for all hybrid assemblies shown in Figure 12B. Similar findings have also been reported for other inorganic nanoparticles/protein moieties.[129-132] Since there was less spectral overlap between the emission peaks of QD1 and QD3, these two QDs were chosen for the coupling with SP1. Figure 12C shows two new emission peaks after combining QD1 and QD3 with SP1. The drop in the emission peak for QD1, in addition to the enhancement in QD3 emission, was demonstrative of a nonradiative energy transfer relayed by the self-assembled protein.

5. CONCLUSIONS AND FUTURE PERSPECTIVES

There is no question that energy transfer has occurred in many hybrid QD-based systems.[25, 71] These QD heterostructures that are comprised of either molecular or biological components have demonstrated promising success in various applications, such as in sensing, energy, etc. In these heteroassemblies, the photoluminescence of QDs is often quenched or sometimes enhanced at the ensemble level. At the single QD level, the energy donor/acceptor molecules also impact the

"blinking" (photoluminescence intermittency) behavior of individual QDs.[133-135] The appropriate combination of QDs and molecules can potentially suppress or eliminate "blinking" of the single QDs, creating steady emitters. In addition to the traditional FRET and DET mechanisms, the recent findings in TTET between the excitons in QDs and molecular triplets open a new avenue of QD-enabled energy transfer. Despite successful examples demonstrating the potential high efficiency of this process in creating triplet states, the quality of QD surface passivation could largely impact TTET, which is an area worthy of further investigation. Although more recent studies have fixated on single excitons in QDs, multi-excitons can be generated in high quality core/shell QDs that have nanosecond scale lifetimes. We propose that these multi-excitons could also transfer energy to molecular triplets by selecting the ideal QD-molecular triplet combination. The prospect of multi-exciton to triplet energy transfer is an exciting topic that has yet to be explored in the near future.

In the QD/biomolecule constructs, the impact of energy transfer on the QD absorption/photoluminescence properties have been demonstrated in a substantial number of systems.[71, 136] The hybrid QD/biological systems have shown enhanced properties, such as broader absorption compared to that of isolated QDs. The broad absorption can potentially increase the light harvesting efficiency in the hybrid materials. However, the impact of QDs on the spectral features of biological components is much less studied. Moreover, how QDs alter the function of proteins remains an important, yet under investigated topic, especially on the biological activity of proteins. Since there are few studies that concentrate on the influence of QDs on proteins, this limitation can create issues in engineering biomimetic devices, in which the hybrid materials must maintain the desired physical/biological properties and long-term stability for optimal device performance. Therefore, proper ligand functionalization on QD surfaces is essential to fabricate

bio-compatible QDs. In the past years, there have been many chemical and physical methods developed to functionalize the QD surface so that the QDs are anchored to the proteins. Nevertheless, specific attachment of QDs to desired sites on the proteins with well-controlled QD/protein molar ratios is still a challenge and an avenue worth exploring in more detail.

Similar to the favorable properties that QDs possess, multiple biological systems display interesting optical characteristics that can be employed for biomimetic devices. As demonstrated in our own study,[107] the photoactive protein bacteriorhodopsin (BR) exhibits unique optical and physical characteristics, leading to the incorporation of BR into a myriad of device applications.[117] In addition to photoluminescence quenching of the QDs by BR, we observed a modulation in the BR photocycle for multiple QD/BR assemblies. We envisage that the tunability of the BR photocycle would be highly advantageous for protein-based computing applications that depend on the photochromic pairing of the **M** and **bR** photointermediates of the photocycle. We hope that our current findings inspire other research groups to study analogous QD/biological systems and to further elucidate on how the optical properties of the biological components are influenced by QDs.

The results from these fundamental studies on energy transfer in hybrid QD/molecular nanomaterials have laid the foundation for the development of advanced optoelectronic devices that are dependent on hybrid QD assemblies. Overcoming the limitations in energy transfer efficiency concomitant with the stability and reproducibility of current hybrid nanosystems will enable future practical applications of these materials in display, light harvesting, catalysis, and biological sensing and imaging systems.

CONFLICTS OF INTEREST

There are no conflicts to declare.

AUTHOR INFORMATION

Corresponding Author

*Email: jing.zhao@uconn.edu. Phone: 860-486-2443. Fax: 860-486-2981.

ACKNOWLEDGEMENTS

This work was supported in part by the National Science Foundation (CAREER-1554800).

REFERENCES

1 A. Hagfeldt, G. Boschloo, L. Sun, L. Kloo and H. Pettersson, *Chem. Rev.*, 2010, **110**, 6595–6663.

2 J.-J. Kim, J. Lee, S.-P. Yang, H. G. Kim, H.-S. Kweon, S. Yoo and K.-H. Jeong, *Nano Lett.*, 2016, **16**, 2994–3000.

3 E. Fresta, V. Fernández-Luna, P. B. Coto and R. D. Costa, *Adv. Funct. Mater.*, 2018, **28**, 1707011.

4 V. Biju, T. Itoh, A. Anas, A. Sujith and M. Ishikawa, *Anal. Bioanal. Chem.*, 2008, **391**, 2469–2495.

5 P. Alivisatos, *Nat. Biotechnol.*, 2003, **22**, 47–52.

6 B. A. Kairdolf, A. M. Smith, T. H. Stokes, M. D. Wang, A. N. Young and S. Nie, *Annu. Rev. Anal. Chem.*, 2013, **6**, 143–162.

7 G. H. Carey, A. L. Abdelhady, Z. Ning, S. M. Thon, O. M. Bakr and E. H. Sargent, *Chem. Rev.*, 2015, **115**, 12732–12763.

8 A. Kongkanand, K. Tvrdy, K. Takechi, M. Kuno and P. V. Kamat, *J. Am. Chem. Soc.*, 2008, **130**, 4007–4015.

9 S. Jin, H.-J. Son, O. K. Farha, G. P. Wiederrecht and J. T. Hupp, *J. Am. Chem. Soc.*, 2013, **135**, 955–958.

10 Y. Shirasaki, G. J. Supran, M. G. Bawendi and V. Bulović, *Nat. Photonics*, 2012, **7**, 13–23.

11 Y.-Y. Wang, X. Xiang, R. Yan, Y. Liu and F.-L. Jiang, *J. Phys. Chem. C*, 2018, **122**, 1148–1157.

12 L. Dworak, S. Roth and J. Wachtveitl, *J. Phys. Chem. C*, 2017, **121**, 2613–2619.

13 L. Dworak, V. V. Matylitsky, T. Ren, T. Basché and J. Wachtveitl, *J. Phys. Chem. C*, 2014, **118**, 4396–4402.

14 M. S. Kodaimati, K. P. McClelland, C. He, S. Lian, Y. Jiang, Z. Zhang and E. A. Weiss, *Inorg. Chem.*, 2018, **57**, 3659–3670.

15 P. V. Kamat, *Chem. Rev.*, 1993, **93**, 267–300.

16 P. V. Kamat, *J. Phys. Chem. C*, 2008, **112**, 18737–18753.

17 R. D. Harris, S. Bettis Homan, M. Kodaimati, C. He, A. B. Nepomnyashchii, N. K. Swenson, S. Lian, R. Calzada and E. A. Weiss, *Chem. Rev.*, 2016, **116**, 12865–12919.

18 S. Lian, M. S. Kodaimati, D. S. Dolzhnikov, R. Calzada and E. A. Weiss, *J. Am. Chem. Soc.*, 2017, **139**, 8931–8938.

19 J. Zhou, Y. Yang and C.-y. Zhang, *Chem. Rev.*, 2015, **115**, 11669–11717.

20 J. Yao, M. Yang and Y. Duan, *Chem. Rev.*, 2014, **114**, 6130–6178.

21 J. Li and J.-J. Zhu, *Analyst*, 2013, **138**, 2506–2515.

22 D. Geißler, L. J. Charbonnière, R. F. Ziessel, N. G. Butlin, H.-G. Löhmannsröben and N. Hildebrandt, *Angew. Chem., Int. Ed.*, 2010, **49**, 1396–1401.

23 Y. Zheng, S. Gao and J. Y. Ying, *Adv. Mater.*, 2007, **19**, 376–380.

24 H.-Q. Peng, L.-Y. Niu, Y.-Z. Chen, L.-Z. Wu, C.-H. Tung and Q.-Z. Yang, *Chem. Rev.*, 2015, **115**, 7502–7542.

25 S. Kundu and A. Patra, *Chem. Rev.*, 2017, **117**, 712–757.

26 T. Mirkovic, E. E. Ostroumov, J. M. Anna, R. van Grondelle, Govindjee and G. D. Scholes, *Chem. Rev.*, 2017, **117**, 249–293.

27 A. Shamirian, A. Ghai and P. T. Snee, *Sensors*, 2015, **15**, 13028–13051.

28 M. Wu, M. Massey, E. Petryayeva and W. R. Algar, *J. Phys. Chem. C*, 2015, **119**, 26183–26195.

29 S. Saha, D. Majhi, K. Bhattacharyya, N. Preeyanka, A. Datta and M. Sarkar, *Phys. Chem. Chem. Phys.*, 2018, **20**, 9523–9535.

30 A. M. Dennis and G. Bao, *Nano Lett.*, 2008, **8**, 1439–1445.

31 S. Dayal and C. Burda, *J. Am. Chem. Soc.*, 2007, **129**, 7977–7981.

32 M. Sykora, M. A. Petruska, J. Alstrum-Acevedo, I. Bezel, T. J. Meyer and V. I. Klimov, *J. Am. Chem. Soc.*, 2006, **128**, 9984–9985.

33 M. Malicki, K. E. Knowles and E. A. Weiss, *ChemComm*, 2013, **49**, 4400–4402.

34 A. M. Scott, W. R. Algar, M. H. Stewart, S. A. Trammell, J. B. Blanco-Canosa, P. E. Dawson, J. R. Deschamps, R. Goswami, E. Oh, A. L. Huston and I. L. Medintz, *J. Phys. Chem. C*, 2014, **118**, 9239–9250.

35 L. Yuan, W. Lin, K. Zheng and S. Zhu, *Acc. Chem. Res.*, 2013, **46**, 1462–1473.

36 E. Lee, C. Kim and J. Jang, *Chem.: Eur. J.*, 2013, **19**, 10280–10286.

37 E. A. Jares-Erijman and T. M. Jovin, *Nat. Biotechnol.*, 2003, **21**, 1387–1395.

38 T. Förster, *Naturwissenschaften*, 1946, **33**, 166–175.

39 R. M. Clegg, in *Reviews in Fluorescence 2006*, eds. C. D. Geddes and J. R. Lakowicz, Springer US, Boston, MA, 2006, 1–45.

40 R. E. Dale, J. Eisinger and W. E. Blumberg, *Biophys. J.*, 1979, **26**, 161–193.

41 R. E. Dale and J. Eisinger, *Biopolymers*, 1974, **13**, 1573–1605.

42 H. Htoon, M. Furis, S. Crooker, S. Jeong and V. I. Klimov, *Phys. Rev. B*, 2008, **77**, 035328.

43 D. B. Tice, D. J. Weinberg, N. Mathew, R. P. Chang and E. A. Weiss, *J. Phys. Chem. C*, 2013, **117**, 13289–13296.

44 M. Li, S. K. Cushing, Q. Wang, X. Shi, L. A. Hornak, Z. Hong and N. Wu, *J. Phys. Chem. Lett.*, 2011, **2**, 2125–2129.

45 C. S. Yun, A. Javier, T. Jennings, M. Fisher, S. Hira, S. Peterson, B. Hopkins, N. O. Reich and G. F. Strouse, *J. Am. Chem. Soc.*, 2005, **127**, 3115–3119.

46 C. J. Breshike, R. A. Riskowski and G. F. Strouse, *J. Phys. Chem. C*, 2013, **117**, 23942–23949.

47 A. Samanta, Y. Zhou, S. Zou, H. Yan and Y. Liu, *Nano Lett.*, 2014, **14**, 5052–5057.

48 D. L. Dexter, *J. Chem. Phys.*, 1953, **21**, 836–850.

49 D. M. Arias-Rotondo and J. K. McCusker, *Chem. Soc. Rev.*, 2016, **45**, 5803–5820.

50 J. B. Hoffman, H. Choi and P. V. Kamat, *J. Phys. Chem. C*, 2014, **118**, 18453–18461.

51 L. Nienhaus, M. Wu, N. Geva, J. J. Shepherd, M. W. B. Wilson, V. Bulović, T. Van Voorhis, M. A. Baldo and M. G. Bawendi, *ACS Nano*, 2017, **11**, 7848–7857.

52 S. Amemori, Y. Sasaki, N. Yanai and N. Kimizuka, *J. Am. Chem. Soc.*, 2016, **138**, 8702–8705.

53 J. Kim, C. Y. Wong and G. D. Scholes, *Acc. Chem. Res.*, 2009, **42**, 1037–1046.

54 T. N. Singh-Rachford and F. N. Castellano, *Coord. Chem. Rev.*, 2010, **254**, 2560–2573.

55 J. P. Mailoa, A. J. Akey, C. B. Simmons, D. Hutchinson, J. Mathews, J. T. Sullivan, D. Recht, M. T. Winkler, J. S. Williams, J. M. Warrender, P. D. Persans, M. J. Aziz and T. Buonassisi, *Nat. Commun.*, 2014, **5**, 3011.

56 T. Trupke, M. A. Green and P. Würfel, *J. Appl. Phys.*, 2002, **92**, 4117–4122.

57 K. Shankar, X. Feng and C. A. Grimes, *ACS Nano*, 2009, **3**, 788–794.

58 S. Buhbut, S. Itzhakov, E. Tauber, M. Shalom, I. Hod, T. Geiger, Y. Garini, D. Oron and A. Zaban, *ACS Nano*, 2010, **4**, 1293–1298.

59 H. Choi, P. K. Santra and P. V. Kamat, *ACS Nano*, 2012, **6**, 5718–5726.

60 S. Sadhu, K. K. Haldar and A. Patra, *J. Phys. Chem. C*, 2010, **114**, 3891–3897.

61 B. O. Dabbousi, J. Rodriguez-Viejo, F. V. Mikulec, J. R. Heine, H. Mattoussi, R. Ober, K. F. Jensen and M. G. Bawendi, *J. Phys. Chem. B*, 1997, **101**, 9463–9475.

62 A. P. Alivisatos, W. Gu and C. Larabell, *Annu. Rev. Biomed. Eng.*, 2005, **7**, 55–76.

63 A. L. Rogach, A. Eychmüller, S. G. Hickey and S. V. Kershaw, *Small*, 2007, **3**, 536–557.

64 J. M. Pietryga, R. D. Schaller, D. Werder, M. H. Stewart, V. I. Klimov and J. A. Hollingsworth, *J. Am. Chem. Soc.*, 2004, **126**, 11752–11753.

65 E. H. Sargent, *Adv. Mater.*, 2005, **17**, 515–522.

66 T. T. Tan, S. T. Selvan, L. Zhao, S. Gao and J. Y. Ying, *Chem. Mater.*, 2007, **19**, 3112–3117.

67 E. A. McArthur, J. M. Godbe, D. B. Tice and E. A. Weiss, *J. Phys. Chem. C*, 2012, **116**, 6136–6142.

68 H. Choi, R. Nicolaescu, S. Paek, J. Ko and P. V. Kamat, *ACS Nano*, 2011, **5**, 9238–9245.

69 J.-H. Yum, P. Walter, S. Huber, D. Rentsch, T. Geiger, F. Nüesch, F. De Angelis, M. Grätzel and M. K. Nazeeruddin, *J. Am. Chem. Soc.*, 2007, **129**, 10320–10321.

70 S. Paek, H. Choi, C. Kim, N. Cho, S. So, K. Song, M. K. Nazeeruddin and J. Ko, *ChemComm*, 2011, **47**, 2874–2876.

71 N. Hildebrandt, C. M. Spillmann, W. R. Algar, T. Pons, M. H. Stewart, E. Oh, K. Susumu, S. A. Díaz, J. B. Delehanty and I. L. Medintz, *Chem. Rev.*, 2017, **117**, 536–711.

72 D. M. Eisele, H. v. Berlepsch, C. Böttcher, K. J. Stevenson, D. A. Vanden Bout, S. Kirstein and J. P. Rabe, *J. Am. Chem. Soc.*, 2010, **132**, 2104–2105.

73 S. Kirstein and S. Daehne, *Int. J. Photoenergy*, 2006, **2006**, 1–21.

74 G. Scheibe, A. Schöntag and F. Katheder, *Naturwissenschaften*, 1939, **27**, 499–501.

75 A. S. Davydov, *Sov. Phys. Usp.*, 1964, 7, 145–178.

76 M. van Burgel, D. A. Wiersma and K. Duppen, *J. Chem. Phys.*, 1995, **102**, 20–33.

77 A. N. Lebedenko, R. S. Grynyov, G. Y. Guralchuk, A. V. Sorokin, S. L. Yefimova and Y. V. Malyukin, *J. Phys. Chem. C*, 2009, **113**, 12883–12887.

78 D. M. Eisele, J. Knoester, S. Kirstein, J. P. Rabe and D. A. V. Bout, *Nat. Nanotechnol.*, 2009, **4**, 658–663.

79 J. L. Lyon, D. M. Eisele, S. Kirstein, J. P. Rabe, D. A. Vanden Bout and K. J. Stevenson, *J. Phys. Chem. C*, 2008, **112**, 1260–1268.

80 B. J. Walker, V. Bulović and M. G. Bawendi, *Nano Lett.*, 2010, **10**, 3995–3999.

81 B. J. Walker, G. P. Nair, L. F. Marshall, V. Bulovic and M. G. Bawendi, *J. Am. Chem. Soc.*, 2009, **131**, 9624–9625.

82 R. J. Ellingson, M. C. Beard, J. C. Johnson, P. Yu, O. I. Micic, A. J. Nozik, A. Shabaev and A. L. Efros, *Nano Lett.*, 2005, **5**, 865–871.

83 C. Wang and E. A. Weiss, *J. Am. Chem. Soc.*, 2016, **138**, 9557–9564.

84 C. Wang and E. A. Weiss, *Nano Lett.*, 2017, **17**, 5666–5671.

85 S. W. Clark, J. M. Harbold and F. W. Wise, *J. Phys. Chem. C*, 2007, **111**, 7302–7305.

86 C. Wang, M. S. Kodaimati, G. C. Schatz and E. A. Weiss, *ChemComm*, 2017, **53**, 1981–1984.

87 F. Xu, X. Ma, C. R. Haughn, J. Benavides, M. F. Doty and S. G. Cloutier, *ACS Nano*, 2011, **5**, 9950–9957.

88 A. P. Litvin, E. V. Ushakova, P. S. Parfenov, A. V. Fedorov and A. V. Baranov, *J. Phys. Chem. C*, 2014, **118**, 6531–6535.

89 F. S. Freyria, J. M. Cordero, J. R. Caram, S. Doria, A. Dodin, Y. Chen, A. P. Willard and M. G. Bawendi, *Nano Lett.*, 2017, **17**, 7665–7674.

90 M. Tabachnyk, B. Ehrler, S. Gélinas, M. L. Böhm, B. J. Walker, K. P. Musselman, N. C. Greenham, R. H. Friend and A. Rao, *Nat. Mater.*, 2014, **13**, 1033–1038.

91 N. J. Thompson, M. W. Wilson, D. N. Congreve, P. R. Brown, J. M. Scherer, T. S. Bischof, M. Wu, N. Geva, M. Welborn and T. Van Voorhis, *Nat. Mater.*, 2014, **13**, 1039–1043.

92 G. D. Scholes, *Adv. Funct. Mater.*, 2008, **18**, 1157–1172.

93 C. Mongin, S. Garakyaraghi, N. Razgoniaeva, M. Zamkov and F. N. Castellano, *Science*, 2016, **351**, 369–372.

94 M. Wu, D. N. Congreve, M. W. Wilson, J. Jean, N. Geva, M. Welborn, T. Van Voorhis, V. Bulović, M. G. Bawendi and M. A. Baldo, *Nat. Photonics*, 2016, **10**, 31–34.

95 J. H. Warner, E. Thomsen, A. R. Watt, N. R. Heckenberg and H. Rubinsztein-Dunlop, *Nanotechnology*, 2004, **16**, 175–179.

96 Z. Q. You and C. P. Hsu, *Int. J. Quantum Chem.*, 2014, **114**, 102–115.

97 J. A. Bender, E. K. Raulerson, X. Li, T. Goldzak, P. Xia, T. Van Voorhis, M. L. Tang and S. T. Roberts, *J. Am. Chem. Soc.*, 2018, **140**, 7543–7553.

98 S. Garakyaraghi, C. Mongin, D. B. Granger, J. E. Anthony and F. N. Castellano, *J. Phys. Chem. Lett.*, 2017, **8**, 1458–1463.

99 B. J. Walker, A. J. Musser, D. Beljonne and R. H. Friend, *Nat. Chem.*, 2013, **5**, 1019–1024.

100 Z. Xu, F. Gao, E. A. Makarova, A. A. Heikal and V. N. Nemykin, *J. Phys. Chem. C*, 2015, **119**, 9754–9761.

101 M. Werwie, X. Xu, M. Haase, T. Basché and H. Paulsen, *Langmuir*, 2012, **28**, 5810–5818.

102 K. Gundlach, M. Werwie, S. Wiegand and H. Paulsen, *Biochim. Biophys. Acta, Bioenerg.*, 2009, **1787**, 1499–1504.

103 Y. Yoneda, T. Noji, T. Katayama, N. Mizutani, D. Komori, M. Nango, H. Miyasaka, S. Itoh, Y. Nagasawa and T. Dewa, *J. Am. Chem. Soc.*, 2015, **137**, 13121–13129.

104 O. Hassan Omar, S. la Gatta, R. R. Tangorra, F. Milano, R. Ragni, A. Operamolla, R. Argazzi, C. Chiorboli, A. Agostiano, M. Trotta and G. M. Farinola, *Bioconjugate Chem.*, 2016, **27**, 1614–1623.

105 A. O. Govorov, *Adv. Mater.*, 2008, **20**, 4330–4335.

106 I. Nabiev, A. Rakovich, A. Sukhanova, E. Lukashev, V. Zagidullin, V. Pachenko, Y. P. Rakovich, J. F. Donegan, A. B. Rubin and A. O. Govorov, *Angew. Chem., Int. Ed.*, 2010, **49**, 7217–7221.

107 T. J. Wax, J. A. Greco, S. Chen, N. L. Wagner, J. Zhao and R. R. Birge, *Nano Res.*, 2019, **12**, 365–373.

108 J. A. Stuart and R. R. Birge, in *Biomembranes*, ed. A. G. Lee, JAI Press, London, 2A, 1996, 33–140.

109 R. H. Lozier, W. Niederberger, R. A. Bogomolni, S. Hwang and W. Stoeckenius, *Biochim. Biophys. Acta, Bioenerg.*, 1976, **440**, 545–556.

110 J. K. Lanyi, *Annu. Rev. Physiol.*, 2004, **66**, 665–688.

111 S. Hayashi, E. Tajkhorshid and K. Schulten, *Biophys. J.*, 2002, **83**, 1281–1297.

112 K. Edman, P. Nollert, A. Royant, H. Beirhali, E. Pebay-Peyroula, J. Hajdu, R. Neutze and E. M. Landau, *Nature*, 1999, **401**, 822–826.

113 S. P. Balashov, *Biochim. Biophys. Acta, Bioenerg.*, 2000, **1460**, 75–94.

114 A. Rakovich, I. Nabiev, A. Sukhanova, V. Lesnyak, N. Gaponik, Y. P. Rakovich and J. F. Donegan, *ACS Nano*, 2013, **7**, 2154–2160.

115 S. Y. Zaitsev, E. P. Lukashev, D. O. Solovyeva, A. A. Chistyakov and V. A. Oleinikov, *Colloids Surf. B*, 2014, **117**, 248–251.

116 A. Rakovich, A. Sukhanova, N. Bouchonville, E. Lukashev, V. Oleinikov, M. Artemyev, V. Lesnyak, N. Gaponik, M. Molinari, M. Troyon, Y. P. Rakovich, J. F. Donegan and I. Nabiev, *Nano Lett.*, 2010, **10**, 2640–2648.

117 R. R. Birge, N. B. Gillespie, E. W. Izaguirre, A. Kusnetzow, A. F. Lawrence, D. Singh, Q. W. Song, E. Schmidt, J. A. Stuart, S. Seetharaman and K. J. Wise, *J. Phys. Chem. B*, 1999, **103**, 10746–10766.

118 S. Zhang, D. M. Marini, W. Hwang and S. Santoso, *Curr. Opin. Chem. Biol.*, 2002, **6**, 865–871.

119 H. Mattoussi, J. M. Mauro, E. R. Goldman, G. P. Anderson, V. C. Sundar, F. V. Mikulec and M. G. Bawendi, *J. Am. Chem. Soc.*, 2000, **122**, 12142–12150.

120 R. Venerando, G. Miotto, M. Magro, M. Dallan, D. Baratella, E. Bonaiuto, R. Zboril and F. Vianello, *J. Phys. Chem. C*, 2013, **117**, 20320–20331.

121 H. Sun, L. Miao, J. Li, S. Fu, G. An, C. Si, Z. Dong, Q. Luo, S. Yu, J. Xu and J. Liu, *ACS Nano*, 2015, **9**, 5461–5469.

122 X. Li, Y. Bai, Z. Huang, C. Si, Z. Dong, Q. Luo and J. Liu, *Nanoscale*, 2017, **9**, 7991–7997.

123 Y. Bai, Q. Luo and J. Liu, *Chem. Soc. Rev.*, 2016, **45**, 2756–2767.

124 E. R. Ballister, A. H. Lai, R. N. Zuckermann, Y. Cheng and J. D. Mougous, *Proc. Natl. Acad. Sci.*, 2008, **105**, 3733–3738.

125 H. Kitagishi, Y. Kakikura, H. Yamaguchi, K. Oohora, A. Harada and T. Hayashi, *Angew. Chem.*, 2009, **121**, 1297–1300.

126 I. Medalsy, O. Dgany, M. Sowwan, H. Cohen, A. Yukashevska, S. G. Wolf, A. Wolf, A. Koster, O. Almog, I. Marton, Y. Pouny, A. Altman, O. Shoseyov and D. Porath, *Nano Lett.*, 2008, **8**, 473–477.

127 A. Khoutorsky, A. Heyman, O. Shoseyov and M. E. Spira, *Nano Lett.*, 2011, **11**, 2901–2904.

128 L. Miao, J. Han, H. Zhang, L. Zhao, C. Si, X. Zhang, C. Hou, Q. Luo, J. Xu and J. Liu, *ACS Nano*, 2014, **8**, 3743–3751.

129 L. Wang, L. Wang, C. Zhu, X. Wei and X. Kan, *Anal. Chim. Acta*, 2002, **468**, 35–41.

130 N. N. Mamedova, N. A. Kotov, A. L. Rogach and J. Studer, *Nano Lett.*, 2001, **1**, 281–286.

131 K.-i. Hanaki, A. Momo, T. Oku, A. Komoto, S. Maenosono, Y. Yamaguchi and K. Yamamoto, *Biochem. Biophys. Res. Commun.*, 2003, **302**, 496–501.

132 L.-Y. Wang, X.-W. Kan, M.-C. Zhang, C.-Q. Zhu and L. Wang, *Analyst*, 2002, **127**, 1531–1534.

133 S. Jin, J.-C. Hsiang, H. Zhu, N. Song, R. M. Dickson and T. Lian, *Chem. Sci.*, 2010, **1**, 519–526.

134 S. Jin, N. Song and T. Lian, *ACS Nano*, 2010, **4**, 1545–1552.

135 N. Song, H. Zhu, S. Jin, W. Zhan and T. Lian, *ACS Nano*, 2011, **5**, 613–621.

136 E. M. Conroy, J. J. Li, H. Kim and W. R. Algar, *J. Phys. Chem. C*, 2016, **120**, 17817–17828.

TABLE OF CONTENTS FIGURE

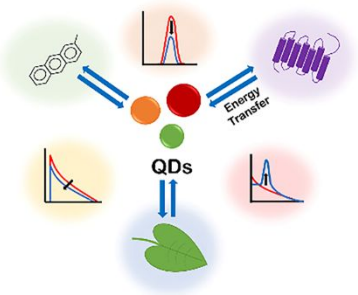

The impact of energy transfer processes on the optical profiles of heteroassemblies with quantum dots as a nano-scaffold are highlighted.